# Supporting Information

# Ultraviolet Photolysis of Acetaldehyde in Clathrate Hydrate Reveals Cage-Controlled Reactivity

*Gaurav Vishwakarma[1], Soham Chowdhury[1], Rajnish Kumar[2,3*], and Thalappil Pradeep[1,3*]*

[1]DST Unit of Nanoscience (DST UNS) and Thematic Unit of Excellence (TUE), Department of Chemistry, Indian Institute of Technology Madras, Chennai 600036, India

[2]Department of Chemical Engineering, Indian Institute of Technology Madras, Chennai 600036, India

[3]International Centre for Clean Water, IIT Madras Research Park, Chennai 600113, India

**Corresponding authors**

***Email:** pradeep@iitm.ac.in, rajnish@iitm.ac.in*

This PDF file includes:
Experimental section (pages S2-S5)
Figure S1 to S4 (pages S6-S10)
Tables S1and S2 (Pages S3 and S7)
References (pages S11-12)

## Experimental Section

### Experimental Setup

The preparation of ice samples, subsequent photolysis, and data acquisition were carried out using a custom-built ultrahigh vacuum (UHV) setup (Figure 1a), detailed in previous reports.[1–3] This setup included a stainless steel UHV chamber with a base pressure of ~$10^{-10}$ mbar, a metal substrate connected to a helium cryocooler, and a gas inlet system. The UHV chamber was equipped with reflection absorption infrared spectroscopy (RAIRS), temperature-programmed desorption (TPD) mass spectrometry, $Cs^+$-based secondary ion mass spectrometry (SIMS), low-energy ion scattering (LEIS) mass spectrometry, and a vacuum ultraviolet (VUV) lamp. UHV was maintained by multiple turbomolecular pumps, which were backed by oil-free diaphragm pumps (Pfeiffer Vacuum). The metal substrate, a highly polished single-crystal Ru(0001), was mounted on the cold end of the helium cryostat (Coldedge Technologies) and was integrated with a precision x-y-z-θ sample manipulator. Temperature control and monitoring were through a Lakeshore Model 336 temperature controller, which utilized a 25 Ω resistive heater, covering a temperature range of 8–1000 K. Temperature measurements were performed using a K-type thermocouple and a platinum sensor, providing an accuracy of ±0.5 K. The gas inlet system was equipped with two high-precision all-metal leak valves for precise control of vapor deposition.

### Materials and Reagents

For all experiments, acetaldehyde (anhydrous, ≥99.5% purity, Sigma-Aldrich) and ultrapure Millipore water (18.2 MΩ cm resistivity) were utilized. The liquid samples were placed in vacuum-sealed test tubes and further purified through repeated freeze-pump-thaw cycles.

### Sample Preparation

Prior to each sample preparation, the Ru(0001) substrate was cleaned by heating it to 400 K multiple times. Thin ice films were then prepared by vapor deposition on the pre-cooled Ru(0001) substrate. Two separate gas inlets, one exclusively for water and the other for

acetaldehyde, were utilized to introduce vapors into the UHV chamber for backfilling. The purity and ratio of acetaldehyde and water were confirmed using a residual gas analyzer during vapor deposition. In the current work, deposition coverage was measured in monolayers (ML) with an assumption that $1.33 \times 10^{-6}$ mbar s equals 1 ML, which is estimated to contain ~$1.1 \times 10^{15}$ molecules $cm^{-2}$, based on previous studies.[2,4–6]

**Determination of the Column Density (*N*)**

The column densities of reactants and photoproducts were determined using a widely applied method:[1,7]

$$N_M = \frac{S_M}{A_M}$$

where $N_M$ represents the column density of molecule M in $cm^{-2}$, $S_M$ is the integrated area of the specific IR band of molecule *M*, and $A_M$ is the band strength for the same band in cm $molecule^{-1}$. For example, values of acetaldehyde column densities ($N_{CH_3CHO}$) were calculated as $N_{CH_3CHO} = \frac{S_{CH_3CHO}}{A_{CH_3CHO}}$, where $S_{CH_3CHO}$ represents the integrated area of the 1350 $cm^{-1}$ band and $A_{CH_3CHO}$ is $4.5 \times 10^{-18}$ cm $molecule^{-1}$.[8,9] The column densities of various photoproducts were estimated similarly. Specific IR bands and their associated band strengths used for these calculations are listed in **Table S1**.

**Table S1.** Characteristic bands and corresponding band strengths of various photoproducts. Band strength values are employed from multiple studies.[9–12]

| Species | Bands ($cm^{-1}$) | Assignment | Band strength (cm $molecule^{-1}$) |
|---|---|---|---|
| $CH_3CHO$ | 1350 | $CH_3$ deform | $7.1 \times 10^{-18}$ |
| CO | 2136 | C=O stretch | $1.1 \times 10^{-17}$ |
| $CO_2$ | 2343 | C=O asym. stretch | $7.6 \times 10^{-17}$ |
| $CH_4$ | 1304 | $CH_2$ bend | $8.0 \times 10^{-18}$ |
| $H_2CCO$ | 2129 | C=O stretch | $1.2 \times 10^{-16}$ |
| $CH_3OH$ | 1017 | C-O stretch | $1.8 \times 10^{-17}$ |
| $CH_3CH_2OH$ | 1050 | C-O stretch | $7.3 \times 10^{-18}$ |

**Normalization of photoproduct column densities**: Because the initial amount of acetaldehyde may differ between runs and among the three samples (pure acetaldehyde, acetaldehyde+$H_2O$ mixed ice, and acetaldehyde clathrate hydrate, ACH), the absolute amount of photoproducts formed could not be compared directly. To account for this, the fraction of each photoproduct produced was normalized to the initial amount of acetaldehyde present in the corresponding sample.

The normalized column density of a photoproduct was calculated as,

$$N_{p,norm} = \left(\frac{S_{p,t} - S_{p,0}}{S_{a,0}}\right) \times \frac{1}{A_p}$$

where

$S_{p,t}$ is the integrated area of the selected IR band of the photoproduct at time $t$,

$S_{p,0}$ is the integrated area of the same band at $t = 0$,

$S_{a,0}$ is the integrated area of the acetaldehyde band at $t = 0$ for the corresponding sample, and

$A_p$ is the band strength of the selected band of the photoproduct.

This normalization accounts for differences in the initial acetaldehyde amounts and allows direct comparison of photoproduct formation across the three systems.

**Retention calculation:** The percentage retention of each photoproduct (Figure 4a) was calculated relative to the total acetaldehyde depleted during photolysis as,

$$\%\text{Retention} = \frac{N_p}{N_{a,0} - N_{a,t}} \times 100$$

Where $N_p$ is the column density of the photoproduct, and

$N_{a,0} - N_{a,t}$ represents the change in the acetaldehyde column density during photolysis.

**Experimental Protocol**

Thin ice films of pure acetaldehyde, a mixture of acetaldehyde and $H_2O$, and ACH were prepared as described in our previous study.[13] For instance, for the preparation of ~300 ML acetaldehyde+$H_2O$ mixture at a 1:2 ratio, the inlet pressure for acetaldehyde and $H_2O$ was maintained at ~$2.5\times10^{-7}$ mbar each for 10 min, factoring in ion-gauge sensitivity values of ~2.0 for acetaldehyde and ~1.0 for $H_2O$.[14] For the preparation of ACH, as reported in our previous study,[13] the acetaldehyde+$H_2O$ (1:2) mixed ice, created at 10 K, was heated to 137 K. Heating the sample to 137 K ensures formation of ACH and removal of free acetaldehyde from ice matrix. The formation of ACH was confirmed by RAIRS, indicated by the emergence of the 1734 $cm^{-1}$ peak, as shown in Figure S1. It should be noted that acetaldehyde typically occupies the large $5^{12}6^4$ cages of CH structure II (sII).[15] After preparing ACH at 137 K, ice sample was cooled to 10 K for photolysis. Following the sample preparation, pure acetaldehyde, acetaldehyde+$H_2O$ (1:2) mixed ice, and ACH were photolyzed at 10 K by VUV exposure. RAIRS was used to examine ice samples before and after VUV exposure at regular intervals. It is worth noting that pure acetaldehyde, and acetaldehyde+$H_2O$ mixed ice were directly created by vapor deposition at 10 K, however, ACH samples were created by heating acetaldehyde+$H_2O$ (1:2) mixture to 137 K and cooling it back to 10 K.

**VUV Lamp**

We have recently added a VUV lamp to our existing UHV chamber to carry out photolysis of molecular ices.[1,2,16] The UV light source is a deuterium lamp (McPherson, Model 634, $MgF_2$ window with a cut-off at ~114 nm/10.87 eV, 30 W) of VUV range, 115-400 nm. The emission spectrum of the Model 634 deuterium lamp, as provided by McPherson, is shown in Figure 1b. The VUV lamp was differentially pumped with a turbomolecular pump (Pfeiffer Vacuum). The estimated average photon flux reaching the ice sample was $\sim 6 \times 10^{12}$ photons $cm^{-2}$ $s^{-1}$.[1,16]

**RAIRS Setup**

RAIR spectra were collected by Bruker Vertex 70 FT-IR spectrometer in the range of 4000-550 $cm^{-1}$ with a spectral resolution of 2 $cm^{-1}$. Each RAIR spectrum was averaged over 512 scans to ensure a better signal-to-noise ratio. The RAIRS setup, connected to the UHV chamber via an IR-transparent ZnSe viewport, consists of an FT-IR spectrometer and a liquid nitrogen-cooled mercury cadmium telluride (MCT) detector. For experiments, the IR beam was focused on the ice sample at an incident angle of 80° ± 7°, and the reflected beam was recorded using the MCT detector. The IR beam outside the UHV chamber was purged with dry $N_2$ to avoid interference with atmospheric gases.

**Supporting Information 1**

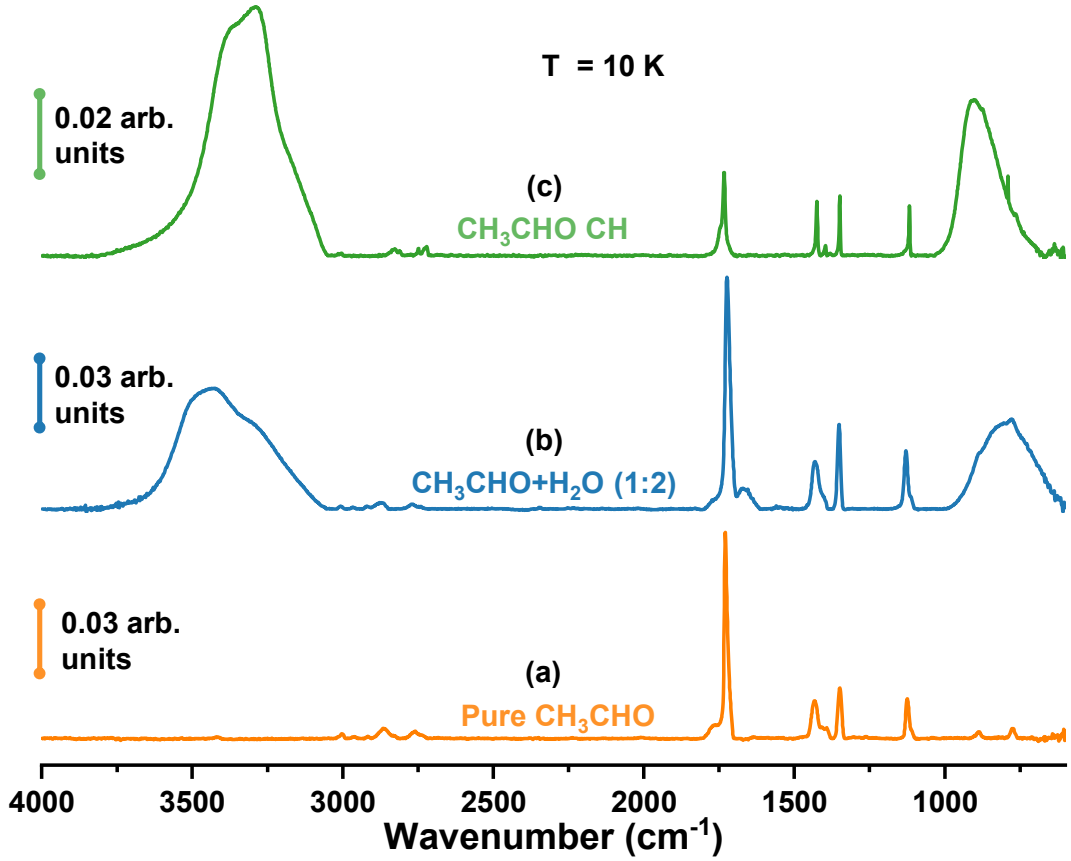


**Figure S1.** Full range RAIR spectra of (a) ~100 ML pure acetaldehyde, (b) ~300 ML acetaldehyde+$H_2O$ (1:2) mixed ice, and (c) ACH at 10 K before VUV photolysis. The ACH sample was prepared by annealing ~300 ML of acetaldehyde+$H_2O$ (1:2) mixed ice from 10 to 137 K. Then it was cooled back to 10 K for photolysis. Pure acetaldehyde ice and acetaldehyde+$H_2O$ (1:2) mixed ice were created directly by vapor deposition on Ru(0001) at 10 K. Peak assignments are listed in Table S2.

**Table S2.** Peak positions of acetaldehyde in pure acetaldehyde, acetaldehyde+$H_2O$ mixed ice and ACH prior VUV photolysis at 10 K, along with new bands observed during VUV photolysis at 10 K. A tick (✓) indicates the presence of the species, while a hyphen (–) denotes its absence. Peak assignments are consistent with the references (ref.) provided in brackets.

| Before photolysis | | | New products observed during VUV photolysis (Ref.) | Position ($cm^{-1}$) and assignments | Pure $CH_3CHO$ | $CH_3CHO$ + $H_2O$ (1:2) | ACH |
|---|---|---|---|---|---|---|---|
| Pure $CH_3CHO$ | $CH_3CHO$ + $H_2O$ (1:2) | ACH ([13]) | | | | | |
| 3003 | 3007 | 3004 | $CO_2$ ([12,17]) | 2340/2343 $\nu_3$ (C=O a-str.) | ✓ | ✓ | ✓ |
| 2961, 2916 | 2966, 2920 | 2829, 2810 | CO ([12,17]) | 2136 a-str. $\nu_1$ (C=O str.) | ✓ | ✓ | ✓ |
| 2864, 2759 | 2873, 2769 | 2748, 2721 | $H_2CCO$ ([9,11]) | 2129 $\nu_2$ (C=O str.) | ✓ | - | - |
| 1774, **1729** | 1774, **1722** | **1734**, 1745 | $CH_3CO$ ([18]) | 1843 $\nu_1$ (C=O str.) | - | ✓ | - |
| 1432, | 1432 | 1425 | $CH_4$ ([10,12]) | 1304 $\nu_4$ (C–H a-bend.) | ✓ | ✓ | ✓ |
| 1408 | 1402 | 1396 | HOCO ([19,20]) | 1261 $\nu_3$ (H–O–C def.) | ✓ | ✓ | ✓ |
| 1391 | 1394 | 1378 | $CH_2OH$ ([21,22]) | 1194 $\nu_5$ (C–O str.) | ✓ | - | - |
| 1348 | 1350 | 1350 | $CH_3OCH_3$ ([23,24]) | 1150 $\nu_5$ (C–O–C a-str.) | ✓ | ✓ | ✓ |
| 1125 | 1128 | 1118 | $HOCH_2CH_2OH$ ([21,24]) | 1088 $\nu_5$ (C–O–H bend.) | ✓ | ✓ | ✓ |
| 887 | 890 | 873 | $CH_3CH_2OH$ ([12,23]) | 1050 $\nu_6$ (C–O str.) | ✓ | ✓ | ✓ |
| 775 | 775 | 765 | $CH_3OH$ ([12,25]) | 1017 $\nu_6$ (C–O str.) | - | ✓ | - |

## Supporting Information 2

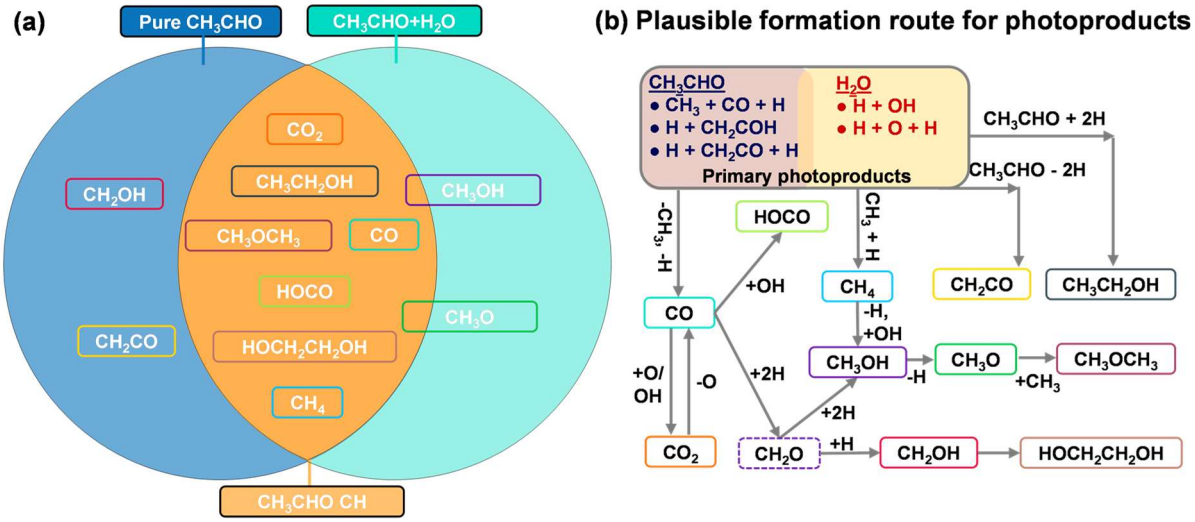


**Figure S2.** (a) Comparison of the photoproducts generated from the photolysis of pure acetaldehyde, acetaldehyde+$H_2O$ (1:2) mixed ice, and ACH at 10 K. (b) Proposed formation pathways for the various photoproducts identified via RAIRS analysis, highlighting the primary photoproducts derived from $CH_3CHO$ and $H_2O$.

## Supporting Information 3

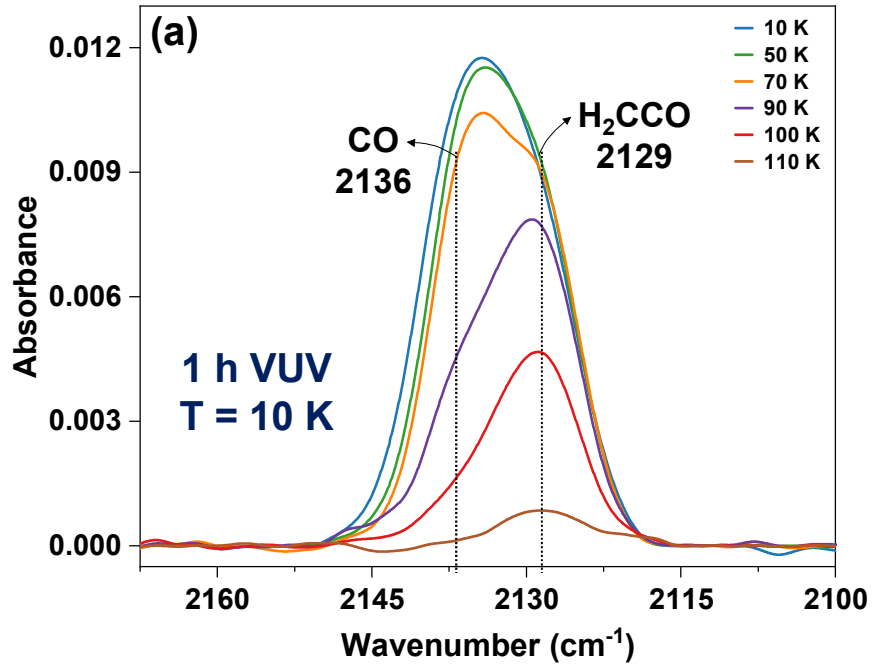


**Figure S3**. Temperature-dependent RAIR spectra of VUV-photolyzed pure acetaldehyde ice (1 h VUV at 10 K), annealed from 10 K to 110 K at 5 K/min, focusing on the C=O stretching region (2167–2100 $cm^{-1}$). At 10 K, a broad peak consisting of components at 2136 $cm^{-1}$ and 2129 $cm^{-1}$ was observed. Upon annealing the sample from 10 to 100 K, the peak at 2136 $cm^{-1}$ vanished, while the peak at 2129 $cm^{-1}$ remained. This indicates that the peak at 2136 $cm^{-1}$ corresponds to CO and the peak at 2129 $cm^{-1}$ corresponds to ketene ($H_2CCO$), as reported in previous studies.[9,11] At 110 K, both peaks disappeared due to the desorption of CO and $H_2CCO$ from the ice matrix.

**Supporting Information 4**

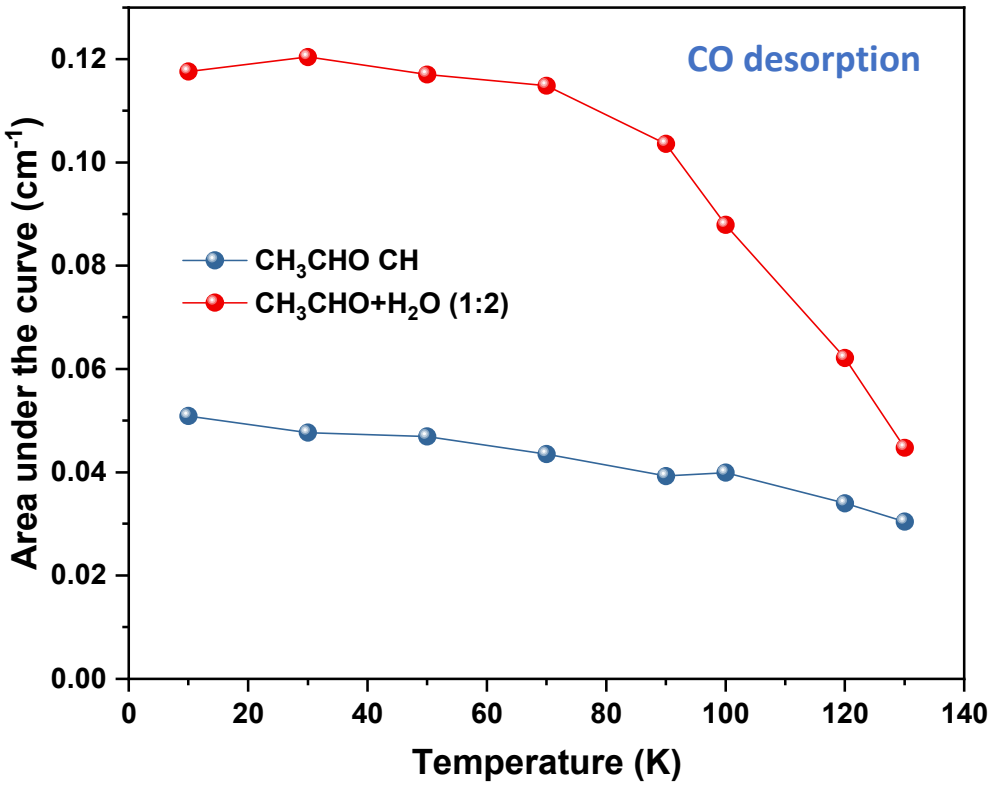


**Figure S4.** Integrated area of the C=O stretching band (2180–2100 $cm^{-1}$) plotted against temperature for the VUV photolyzed ACH sample (blue trace) and the acetaldehyde+$H_2O$ mixed ice (red trace). CO desorption was greater in the mixed ice than in the ACH sample, where CO was trapped within clathrate cages, limiting its release.

## References


(1) Vishwakarma, G.; Malla, B. K.; Kumar, R.; Pradeep, T. Partitioning Photochemically Formed CO2 into Clathrate Hydrate under Interstellar Conditions. *Phys. Chem. Chem. Phys.* **2024**, *26* (22), 16008–16016. https://doi.org/10.1039/D4CP01414F.

(2) Vishwakarma, G.; Malla, B. K.; Reddy, K. S. S. V. P.; Ghosh, J.; Chowdhury, S.; Yamijala, S. S. R. K. C.; Reddy, S. K.; Kumar, R.; Pradeep, T. Induced Migration of CO2 from Hydrate Cages to Amorphous Solid Water under Ultrahigh Vacuum and Cryogenic Conditions. *J. Phys. Chem. Lett.* **2023**, *14*, 2823–2829. https://doi.org/10.1021/acs.jpclett.3c00373.

(3) Bag, S.; Bhuin, R. G.; Methikkalam, R. R. J.; Pradeep, T.; Kephart, L.; Walker, J.; Kuchta, K.; Martin, D.; Wei, J. Development of Ultralow Energy (1-10 EV) Ion Scattering Spectrometry Coupled with Reflection Absorption Infrared Spectroscopy and Temperature Programmed Desorption for the Investigation of Molecular Solids. *Rev. Sci. Instrum.* **2014**, *85* (1), 14103. https://doi.org/10.1063/1.4848895.

(4) Ghosh, J.; Methikkalam, R. R. J.; Bhuin, R. G.; Ragupathy, G.; Choudhary, N.; Kumar, R.; Pradeep, T. Clathrate Hydrates in Interstellar Environment. *Proc. Natl. Acad. Sci. U. S. A.* **2019**, *116* (5), 1526–1531. https://doi.org/10.1073/pnas.1814293116.

(5) Vishwakarma, G.; Malla, B. K.; Methikkalam, R. R. J.; Pradeep, T. Rapid Crystallization of Amorphous Solid Water by Porosity Induction. *Phys. Chem. Chem. Phys.* **2022**, *24* (42), 26200–26210. https://doi.org/10.1039/D2CP02640F.

(6) Vishwakarma, G.; Ghosh, J.; Pradeep, T. Desorption-Induced Evolution of Cubic and Hexagonal Ices in an Ultrahigh Vacuum and Cryogenic Temperatures. *Phys. Chem. Chem. Phys.* **2021**, *23* (41), 24052–24060. https://doi.org/10.1039/D1CP03872A.

(7) Kulikov, M. Y.; Feigin, A. M.; Schrems, O. H2O2 Photoproduction inside H2O and H2O:O2 Ices at 20–140 K. *Sci. Rep.* **2019**, *9* (1). https://doi.org/10.1038/s41598-019-47915-w.

(8) Ibrahim, M.; Guillemin, J.-C.; Chaquin, P.; Markovits, A.; Krim, L. The Significant Role of Water in Reactions Occurring on the Surface of Interstellar Ice Grains: Hydrogenation of Pure Ketene H2C=C=O Ice versus Hydrogenation of Mixed H2C=C=O/H2O Ice at 10 K. *Phys. Chem. Chem. Phys.* **2024**, *26* (5), 4200–4207. https://doi.org/10.1039/D3CP04601J.

(9) Hudson, R. L.; Ferrante, R. F. Quantifying Acetaldehyde in Astronomical Ices and Laboratory Analogues: IR Spectra, Intensities, 13C Shifts, and Radiation Chemistry. *Mon. Not. R. Astron. Soc.* **2020**, *492* (1), 283–293. https://doi.org/10.1093/mnras/stz3323.

(10) Bouilloud, M.; Fray, N.; Bénilan, Y.; Cottin, H.; Gazeau, M.-C.; Jolly, A. Bibliographic Review and New Measurements of the Infrared Band Strengths of Pure Molecules at 25 K: H2O, CO2, CO, CH4, NH3, CH3OH, HCOOH and H2CO. *Mon. Not. R. Astron. Soc.* **2015**, *451* (2), 2145–2160. https://doi.org/10.1093/mnras/stv1021.

(11) Hudson, R. L.; Loeffler, M. J. Ketene Formation in Interstellar ICES: A Laboratory Study. *Astrophys. J.* **2013**, *773* (2), 109. https://doi.org/10.1088/0004-637X/773/2/109.

(12) Martín-Doménech, R.; Muñoz Caro, G. M.; Cruz-Díaz, G. A. Study of the Photon-Induced Formation and Subsequent Desorption of CH3OH and H2CO in Interstellar Ice Analogs. *Astron. Astrophys.* **2016**, *589*, A107–A107. https://doi.org/10.1051/0004-6361/201528025.

(13) Vishwakarma, G.; Malla, B. K.; Chowdhury, S.; Khandare, S. P.; Pradeep, T. Existence of Acetaldehyde Clathrate Hydrate and Its Dissociation Leading to Cubic Ice under Ultrahigh Vacuum and Cryogenic Conditions. *J. Phys. Chem. Lett.* **2023**, *14*

(23), 5328–5334. https://doi.org/10.1021/acs.jpclett.3c01181.
(14) Bartmess, J. E.; Georgiadis, R. M. Empirical Methods for Determination of Ionization Gauge Relative Sensitivities for Different Gases. *Vacuum* **1983**, *33* (3), 149–153. https://doi.org/10.1016/0042-207X(83)90004-0.
(15) Davidson, D. W.; Gough, S. R.; Ripmeester, J. A. Dielectric and Nuclear Magnetic Resonance Characterization of Unstable Clathrate Hydrates of Acetaldehyde and Propionaldehyde. *Can. J. Chem.* **1976**, *54* (19), 3085–3088. https://doi.org/10.1139/v76-439.
(16) Malla, B. K.; Vishwakarma, G.; Chowdhury, S.; Pradeep, T. Vacuum Ultraviolet Photolysis of Condensed Methyl Chloride in Interstellar Model Conditions and Trapping of Intermediates at Intergrain Interfaces. *J. Phys. Chem. C* **2023**, *127* (50), 24149–24157. https://doi.org/10.1021/acs.jpcc.3c05889.
(17) Gerakines, P. A.; Schutte, W. A.; Greenberg, J. M.; van Dishoeck, E. F. The Infrared Band Strengths of H2O, CO and CO2 in Laboratory Simulations of Astrophysical Ice Mixtures. *Astron. Astrophys.* **1995**, *296* (3), 810–818.
(18) Kleimeier, N. F.; Turner, A. M.; Fortenberry, R. C.; Kaiser, R. I. On the Formation of the Popcorn Flavorant 2,3-Butanedione (CH3COCOCH3) in Acetaldehyde-Containing Interstellar Ices. *ChemPhysChem* **2020**, *21* (14), 1531–1540. https://doi.org/10.1002/cphc.202000116.
(19) Milligan, D. E.; Jacox, M. E. Infrared Spectrum and Structure of Intermediates in the Reaction of OH with CO. *J. Chem. Phys.* **1971**, *54* (3), 927–942. https://doi.org/10.1063/1.1675022.
(20) Morley, C.; Smith, I. W. M. Rate Measurements of Reactions of OH by Resonance Absorption. Part 1.—Reactions of OH with NO 2 and NO. *J. Chem. Soc., Faraday Trans. 2* **1972**, *68*, 1016–1030. https://doi.org/10.1039/F29726801016.
(21) Butscher, T.; Duvernay, F.; Danger, G.; Chiavassa, T. Radical-Induced Chemistry from VUV Photolysis of Interstellar Ice Analogues Containing Formaldehyde. *Astron. Astrophys.* **2016**, *593*, A60–A60. https://doi.org/10.1051/0004-6361/201628258.
(22) Jacox, M. E.; Milligan, D. E. Matrix Isolation Study of the Vacuum-Ultraviolet Photolysis of Methanol. *J. Mol. Spectrosc.* **1973**, *47* (1), 148–162. https://doi.org/10.1016/0022-2852(73)90084-2.
(23) Terwisscha Van Scheltinga, J.; Ligterink, N. F. W. W.; Boogert, A. C. A. A.; Van Dishoeck, E. F.; Linnartz, H. Infrared Spectra of Complex Organic Molecules in Astronomically Relevant Ice Matrices: I. Acetaldehyde, Ethanol, and Dimethyl Ether. *Astron. Astrophys.* **2018**, *611*, A35–A35. https://doi.org/10.1051/0004-6361/201731998.
(24) Öberg, K. I.; Garrod, R. T.; van Dishoeck, E. F.; Linnartz, H. Formation Rates of Complex Organics in UV Irradiated CH3OH-Rich Ices. *Astron. Astrophys.* **2009**, *504* (3), 891–913. https://doi.org/10.1051/0004-6361/200912559.
(25) Müller, B.; Giuliano, B. M.; Goto, M.; Caselli, P. Spectroscopic Measurements of CH3OH in Layered and Mixed Interstellar Ice Analogues. *Astron. Astrophys.* **2021**, *652*, A126–A126. https://doi.org/10.1051/0004-6361/202039139.